

# Graph Warp Module: an Auxiliary Module for Boosting the Power of Graph Neural Networks

**Katsuhiko Ishiguro**

Preferred Networks, Inc.  
Tokyo, Japan

k.ishiguro.jp@ieee.org  
ishiguro@preferred.jp

**Shin-ichi Maeda**

Preferred Networks, Inc.  
Tokyo, Japan

ichi@preferred.jp

**Masanori Koyama**

Preferred Networks, Inc.  
Tokyo, Japan

masomatics@preferred.jp

## Abstract

Recently, Graph Neural Networks (GNNs) are trending in the machine learning community as a family of architectures that specializes in capturing the features of graph-related datasets, such as those pertaining to social networks and chemical structures. Unlike for other families of the networks, the representation power of GNNs has much room for improvement, and many graph networks to date suffer from the problem of underfitting. In this paper we will introduce a Graph Warp Module, a supernode-based auxiliary network module that can be attached to a wide variety of existing GNNs in order to improve the representation power of the original networks. Through extensive experiments on molecular graph datasets, we will show that our GWM indeed alleviates the underfitting problem for various existing networks, and that it can even help create a network with the state-of-the-art generalization performance.

## 1 Introduction

Deep neural networks (DNNs) have revolutionized various fields of science, ranging from computer vision, audio/acoustic signal processing, and NLP (e.g. [8, 25, 4]). One major driving force for these successes has been the series of developments of sophisticated architectures with massive function-representation power (e.g. [13, 23]). ResNet [8] in particular has become a hallmark of architectural studies, and its core component, resblock, is widely used in the community today. For the most of the inference tasks to which these architectures are being applied, underfitting seldom becomes a problem. This has been particularly true for image recognition tasks. This is to say that the ability of the recent architectures to *represent* the functions on image dataset is so high that, with appropriate parameter optimization, one can reproduce the input/output relations in the training set almost perfectly.

On the contrary, the representation power of the recently popular new family of neural networks—graph neural networks (GNNs)—is far from the level of the aforementioned architectures. Graph Neural Network is a family of networks specializing in processing the features of graph-structured data (see [33, 29] for comprehensive reviews), and there has been a surge of interest in its application to the analysis of social networks and chemical structure. *Unfortunately, however, loss minimization in GNNs is not yet a trivial task*, and there is much room left for improving the representation power of the network. Thin dashed lines in the left panel and the right panel of Fig. 1 respectively plot the training losses of various GNN architectures against the number of layers and the dimension of the node feature (embedding) vectors. Unlike what we naively expect, the training loss does not decrease monotonically with the number of layers and the dimension of the node vectors.

One solution to this problem is to create a different specialized network for capturing a specific type of features that is essential and common for the domain; this was the approach taken in the development

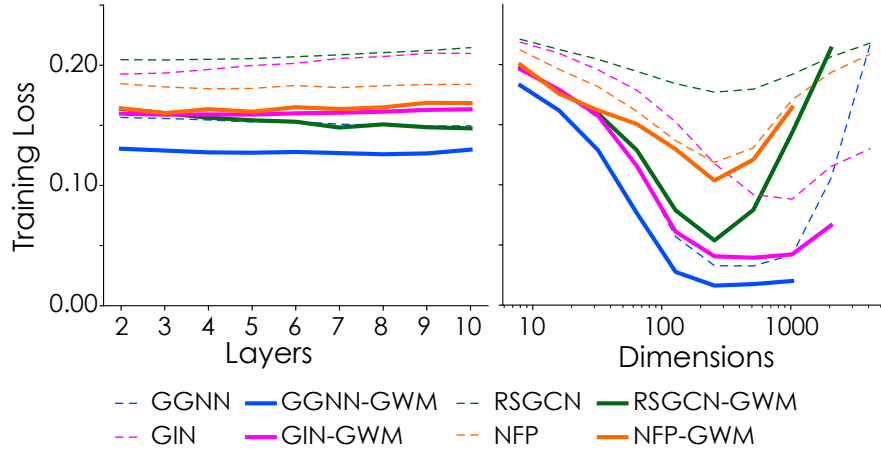


Figure 1: Training losses of various GNN models on a graph dataset (Tox21). The horizontal axis denotes the number of GNN layers (the left panel) or the dimension of the node feature vectors (the right panel). The vertical axis denotes the training loss. Color denotes the GNN model. Thinner dashed lines are the losses of the vanilla GNNs, while thicker solid lines show the losses of the GNNs attached with the proposed Graph Warp Module (“gwm”). Scores are partially unavailable due to memory shortages.

of Convolutional Neural Network (CNN), which were designed to capture shift invariant features in the image dataset. The graph datasets, however, are often highly non-homogeneous in structure, and such endeavor can be futile. At the same time, the existence of a silver-bullet GNN that performs equally well on various tasks is questionable. According to the work of Xu et al. [30], for example, many of the neural message passing type GNNs are theoretically unable to discriminate some graph-isomorphism classes on their own. Moreover, the architecture they proposed as a solution to this problem, (designated as *GIN* in the Fig. 1) is only *asymptotically* as powerful as Weisfeiler-Lehman (WL) graph isomorphism test, and is still yet insufficient in its *practical* representation power.

In this study, we propose graph warp module (GWM), an auxiliary module that can be attached to a generic GNN of various types. Without interfering with the architecture of the original model, GWM can improve the representation power of a GNN of the user’s choice by promoting the information propagation across remote nodes, agnostic to the choice of GNN architecture. Thick solid lines in Fig. 1 plot the training losses of the networks augmented with GWM. As we can see in the figure, the addition of GWM decreases the training loss for all choices of the number of layers and the dimensions of the node feature vectors, for all GNNs. GWM is *modular* in the sense that its I/O is defined independently from the GNN to which it is attached, and the user can improve the representation power of the original GNN by adding just a small segment of code to add the module to the GNN.

There are two key features to our GWM. The first is the use of a *virtual supernode* introduced in [14, 6], which is granted with an ability to communicate with *all* nodes in the graph to promote the message passing. The role given to the supernode is to capture the global properties of the whole graph. Additional messaging paths through the supernode promotes the information propagation between distant nodes, and helps augment the representation power of the GNN with graph-wide representation.

The second feature of our GWM is its attention mechanism [26, 27] and GRU [3]. With trainable weights, the *warp gate* of GWM adjusts the flow of the messages and delivers the message of appropriate strength to each node in the original network. Our contribution is as follows:

1. Through experiments, we demonstrate that current architectures of GNN lack adequate representation power.
2. We introduce GWM, an auxiliary module with a gating mechanism that can be attached to a generic GNN in order to improve the representation power.

3. We show that, with GWM, we can create a GNN model that have state-of-the-art generalization performance.

## 2 Related Work

In this section, we describe the prior relevant works to the construction of GWM and present the background definitions and concepts required to understand its mechanism.

### 2.1 Virtual supernode

In general, most graph neural networks perform inference on graph data of the form  $\{x_i; i \in V\} \subset \mathbf{R}^d$ , where  $V$  is a set of nodes in the graph that are connected through the edge set  $E$ , whose members are represented by pair of adjacent nodes. A common challenge in the study of GNNs is the difficulty in sharing the information among the features of remote nodes, and several studies to date have proposed solutions to this challenge. Hamilton et al. [7] propose graphSAGE which performs pooling-based graph aggregations for large graph computation. Ying et al. [31] propose a way of long-distance information sharing by sequentially pooling the neighborhood vertices.

The approach that we would like to use is the introduction of a supernode, which was originally introduced in Gilmer et al. [6]. By adding a supernode, we can allow a pair of distant nodes to communicate through the supernode in *one hop*. Li et al. [14] also propose a similar idea to learn a graph level representation on a simple GNN. One advantage of this approach is that original GNN retains its structure. However, much concern remains regarding a naive addition of a supernode to a graph, as it can potentially lead to inadvertent “over-smoothing” of the information propagation. For some pairs of nodes, for example, it may be advantageous to delay information sharing. In our study, we therefore make the supernode into a *module equipped with a gated message passing mechanism*, an auxiliary module which enables us to regulate the amount and the type of information that *warps* through the feature space of the supernode.

### 2.2 Message Passing Neural Networks

The supernode in our GWM transmits information using a message passing mechanism, whose name was originally coined by Gilmer et al.[6]. In general, message passing neural networks (MPNN) are defined recursively by composing multiple layers of the form

$$h_{\ell,i} = \mathcal{F}_{\ell}(\{h_{\ell-1,j}; j \in N(i) \cup \{i\}\}) \quad (1)$$

where  $i, j$  are indices of nodes in a graph.  $h_{\ell,i}$  is the feature vector of the node  $i$  at the  $\ell$ th layer,  $N(i)$  is the neighborhoods of the node  $i$ , and  $\mathcal{F}_{\ell}$  is an appropriate choice of function that updates the feature vectors of the previous layer. That is, MPNNs work by literally passing information of each node to its neighbors in a recursive manner. Various ways are proposed for the choice of  $\mathcal{F}$  and for a method of pooling the information of the neighbor of each node. [20, 12, 15, 1, 5].

### 2.3 Gates and Attentions

A seminal MPNN paper [20] assumes that the aggregation weights of  $h_{\ell-1,j}$  is fixed a priori in all  $\mathcal{F}_{\ell}$ . With such architectures, however, one cannot regulate the higher order correlation amongst the outputs from each node. Graph Attention Networks (GATs) [27] introduce a self-attention mechanism [26], which is equipped with a trainable set of weights that controls the importance of edges for each node. Multi-relational attention GCNs [21] take a similar approach, except that they assume edges of different “types” and used different attention weights for each type of edges. The relational graph attention network (RGAT) [2] also builds upon GAT and constructed multiple types of attentions derived from relation-type-wise intermediate node representations. Finally, a GRU [3] is a gating mechanism originally introduced for recurrent neural networks. Gated Graph sequence Neural Networks (GGNN) [15] are the first to apply GRUs to the GNNs, and their method aims to introduce a recurrence relation between successive layers to produce information propagation with greater representation power.

Our GWM is equipped with both multi-relational attention mechanisms and GRUs to grant the module with greater flexibility in transmitting the messages to the graph nodes.

### 3 Graph Warp Module

Our Graph Warp Module (GWM) is made of three building blocks: (1) a supernode, (2) a Transmitter unit, and (3) a Warp gate unit (Fig. 2). In a GWM-augmented graph neural network, information propagates across the graph through *communication* between the supernode and the original (main) GNN at each layer. As shown in Fig. 2, the messages are transmitted to the warp gate from the supernode and the main GNN through the transmitter unit, and the results of the communication are passed back to the module/main network through the warp gate units. In this section, we describe the Graph Warp Module in detail. We begin with the notations of the main network.

#### 3.1 Premise: vanilla GNN and its I/O

Before describing the design of our GWM, we need to present the I/O notation for the family of GNNs we consider in this study, and explain how they will be used when a GWM is attached to a GNN. We denote an arbitrary graph with the edge set  $E$  and the node set  $V$  by  $G = (V, E)$ . We will label the nodes in  $V$  by  $i = 1, 2, \dots, |V|$ , and represent each edge as a pair of nodes in  $V$ . The adjacency matrix  $\mathcal{A} \in \mathbb{R}^{|V| \times |V|}$  is a matrix whose  $i, j$ th entry is the weight assigned to the edge between the node  $i$  and the node  $j$ . Each instance of *data* is passed to the GNN is a set of input feature vectors. We denote an input feature vector associated to node  $i$  as  $x_i$ . The type of GNN that we consider in this study computes the output recursively by applying a composition of smooth functions  $\mathcal{F}_\ell$  to  $x_i$ s. With the understanding that  $x_j = h_{0,j}$ , let  $h_{\ell,i} = \mathcal{F}_{\ell-1,i}(h_{\ell-1,j}; j \in V) \in \mathbb{R}^d$  be the vector of features to be assigned to the  $i$ th node by the  $\ell$ th layer of the GNN. When the GNN is operating on its own without the attachment of a GWM, the GNN updates a feature vector by  $h_{\ell,i} = \mathcal{F}_{\ell-1,i}(h_{\ell-1,j}; j \in V) \in \mathbb{R}^d$ . Finally, the GNN reports some form of the aggregation of  $\{h_{L,i}; i \in V\}$  as the final Readout output.

When a GWM is attached to the GNN, the main GNN is requested to report  $\mathcal{F}_{\ell-1,i}(h_{\ell-1,j}; j \in V) \in \mathbb{R}^d$  as the message from the  $\ell - 1$ th main layer to the module, where it is treated as an element in the *intermodule hyperspace* and is mixed with the transmission from the supernode. The GWM will return the mixed message  $h_\ell$  back to the  $\ell$ th layer of the main GNN. At the same time, the GWM requests a transmission message from the main to the  $\ell$ th supernode. The module will mix the transmission and the message from the  $\ell - 1$ th supernode, and return the mixed message  $g_\ell$  to the  $\ell$ th supernode. When a GWM is attached, the final output is produced by aggregating  $\{h_{L,i}; i \in V\}$  and  $g_L$ .

#### 3.2 Supernode

A supernode is a special node that is connected to nodes in the original graph to promote global information propagation across the network (Fig. 2). A supernode is to be prepared for each  $\ell$ th layer of the main GNN, and we would associate a feature vector  $g_\ell$  to the supernode at the  $\ell$ th layer. At each layer, the transmitter requests from the supernode: (1) a message  $\mathcal{G}_\ell(g_\ell)$  for the  $\ell + 1$ th layer and (2) a transmission to the main network, where  $\mathcal{G}_\ell$  is an appropriate choice of smooth function.

Because a supernode is a superficial variable, we must initialize  $g_0$  manually. For instance, we can use some form of aggregation of the global graph features (e.g. number of nodes or edges, graph diameter, girth, cycle number, min, max, histogram, or average of input node features, . . .). A detailed example of the aggregated feature is presented in the appendix.

#### 3.3 Transmitter Unit

The transmitter unit handles the communications between the main module and the GWM (Fig. 3). The transmitter module is responsible for translating the messages from the recipient into a form that can be mixed in the intermodule hyperspace. We will use multiple types of messages and thus use a separate attention mechanism for each type of message. Before transmitting messages from the main GNN to the supernode, the transmitter uses  $K$ -head attention mechanism to aggregate the messages of each type. We enumerate the components included therein:

- $m_{\ell,k}^{\text{main} \rightarrow \text{super}}$ : aggregated message of head  $k$  from the main GNN to the supernode at layer  $\ell$ .

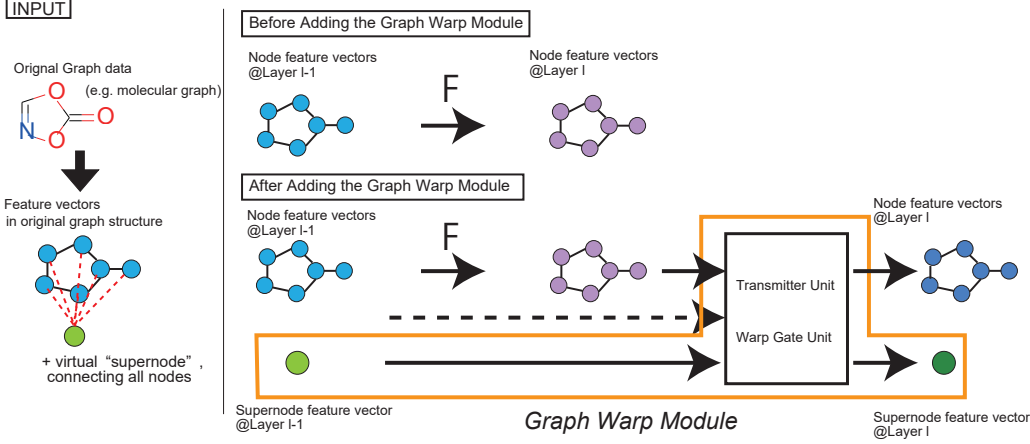


Figure 2: The overview of the proposed Graph Warp Module (GWM). A GWM consists of a virtual supernode, a transmitter unit, and a warp gate unit. A GWM can be added to the original network as an auxiliary module. At each layer, the supernode and the main network communicate through the transmitter unit and the warp gate unit.

- $h_{\ell}^{\text{main} \rightarrow \text{super}}$ : transmission from the the main GNN to the supernode, derived from  $m_{\ell,k}^{\text{main} \rightarrow \text{super}}$ .
- $g_{\ell}^{\text{super} \rightarrow \text{main}}$ : transmission from the supernode to the main at layer  $\ell$ .

The transmissions are to be constructed from the following set of equations. For a vector  $v$ , we use  $v_{m:n} \in \mathbb{R}^{(m-n)d}$  to denote the concatenation of the vectors  $v_m, v_{m+1}, \dots \in \mathbb{R}^d$ . Throughout, we use capital letters to denote the coefficients that are trainable.

$$h_{\ell}^{\text{main} \rightarrow \text{super}} = \tanh \left( W_{\ell} m_{\ell,1:k}^{\text{main} \rightarrow \text{super}} \right) \in \mathbb{R}^{D'}, \quad (2)$$

$$m_{\ell,k}^{\text{main} \rightarrow \text{super}} = \sum_i \alpha_{\ell,i,k} U_{\ell,k} h_{\ell-1,i} \in \mathbb{R}^{D'}, \quad (3)$$

$$\alpha_{\ell,i,k} = \text{softmax} \left( a \left( h_{\ell-1,i}, g_{\ell-1}; A_{\ell,k} \right) \right) \in (0, 1), \quad (4)$$

$$a \left( h_{\ell-1,i}, g_{\ell-1}; A_{\ell,k} \right) := h_{\ell-1,i}^T A_{\ell,k} g_{\ell-1}, \quad (5)$$

where  $\alpha_{\ell,i,k}$  denotes an attention weight of the  $i$ th node at the  $k$ th head (type) and the  $\ell$ th layer.

The transmission from the supernode to the main is simply given by:

$$g_{\ell}^{\text{super} \rightarrow \text{main}} = \tanh \left( F_{\ell} g_{\ell-1} \right) \in \mathbb{R}^D. \quad (6)$$

There is no analogue of  $m$  for the supernode because we are not considering a set of messages of different types to be transmitted from the supernode.

### 3.4 Warp Gate

The warp gate is responsible for merging the transmitted messages and for passing the results to the supernode and the main network through self recurrent units. The gate uses *warp gate coefficients* to control the mixing-rate of the messages. The components of the Warp Gate are:

- $h_{\ell}^0$ : inputs to the GRU unit at  $\ell$ th layer that transmits the message to the main GNN.
- $g_{\ell}^0$ : inputs to the GRU unit at  $\ell$ th layer that transmits the message to the supernode.
- $\hat{g}_{\ell}$ : the message  $\mathcal{G}_{\ell-1} (g_{\ell-1}) \in \mathbb{R}^{D'}$  from the  $\ell - 1$ th supernode, where  $\mathcal{G}$  is an appropriate smooth function with outputs in the intermodule hyperspace.

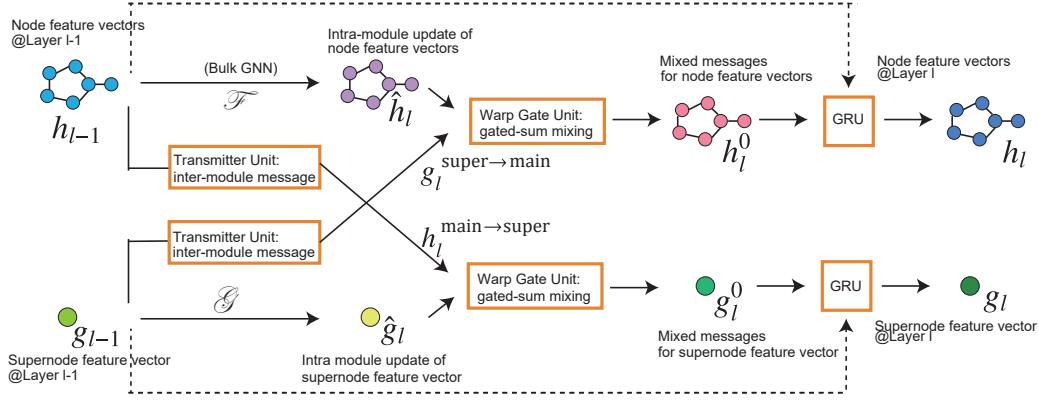


Figure 3: Details of the GWM computations.

- $\hat{h}_{\ell,i}$ : the message  $\mathcal{F}_{\ell-1,i}(h_{\ell-1,k}; k \in V) \in \mathbb{R}^D$  from the  $\ell - 1$ th layer of the main network, expressed in the intermodule hyperspace.
- $z_{\ell,i}$ : tensor of warp gate coefficients for the transmission from the supernode to the main GNN.
- $z_{\ell,i}^{(S)}$ : tensor of warp gate coefficients for the transmission from the main GNN to the supernode.

The module then mixes the transmissions and the messages from the previous layer by applying the following equations:

$$h_{\ell,i}^0 = (1 - z_{\ell,i}) \odot \hat{h}_{\ell-1,i} + z_{\ell,i} \odot g_{\ell}^{\text{super} \rightarrow \text{main}} \in \mathbb{R}^D, \quad (7)$$

$$z_{\ell,i} = \sigma \left( H_{\ell} \tilde{h}_{\ell,i} + G_{\ell} g_{\ell}^{\text{super} \rightarrow \text{main}} \right), \quad (8)$$

$$g_{\ell}^0 = z_{\ell}^{(S)} \odot h_{\ell}^{\text{main} \rightarrow \text{super}} + (1 - z_{\ell}^{(S)}) \odot \hat{g}_{\ell} \in \mathbb{R}^{D'}, \quad (9)$$

$$z_{\ell}^{(S)} = \sigma \left( H_{\ell}^{(S)} h_{\ell}^{\text{main} \rightarrow \text{super}} + G_{\ell}^{(S)} \hat{g}_{\ell} \right), \quad (10)$$

where  $\sigma$  is a nonlinear function whose range lies in  $[0, 1]$ . Finally, the Warp Gate returns the mixed messages to the main GNN and the supernode through gated recurrent units:

$$h_{\ell,i} = \mathbf{GRU} \left( h_{\ell-1,i}, h_{\ell,i}^0 \right) \in \mathbb{R}^D, \quad (11)$$

$$g_{\ell} = \mathbf{GRU} \left( g_{\ell-1}, g_{\ell}^0 \right) \in \mathbb{R}^{D'}. \quad (12)$$

## 4 Experiments

In this section, we present our experimental results on multiple molecular graph datasets in MoleculeNet [28]. We test the efficacy of the GWM for classification tasks and regression tasks. The datasets in MoleculeNet are described in SMILES format, which admits the graph representations we described above. For the details for the dataset and its format, please see [28]. Other details concerning experiments are presented in the appendix.

### 4.1 Setups

#### 4.1.1 Datasets

For the regression tasks, we used the QM9 dataset [19, 18] and the Lipophilicity (LIPO) dataset for the graph regression task. QM9 is a dataset with numerical labels, and contains about 133K drug-like molecules with 12 important chemical-energetic, electronic, and thermodynamic properties, such

as HOMO, LUMO, and electron gaps. The Lipophilicity (LIPO) dataset is another numeric-valued dataset, containing the solubility values of roughly 4K drug molecules. Each instance of data in these datasets is a pair of a molecular graph and a numerical value(s): the 12 chemical properties in the QM9 dataset, and the solubility in the LIPO dataset. For both datasets, the regression task is to predict the numerical value(s) from the molecular graph. We used the train/validation/test data splits of the “scaffold” type, which is considered by the [19, 18] as the most difficult splitting type for test predictions.

In all relevant experiments, all the target chemical values of the QM9 and LIPO datasets were normalized to have zero-mean and unit variance. We evaluated the performance of the models using the mean absolute errors (MAEs).

For the classification task, we used the Tox21 and the HIV datasets. The Tox21 dataset contains about 8K pairs of molecular graph and 12 dimensional binary vector that represents the experimental outcomes of toxicity measurements on 12 different targets. The HIV dataset contains roughly 42K pairs of molecular graph and binary label that represents the medicinal effect of the molecule. For these datasets, the classification task is to predict the binary labels from the molecular graph. For these tasks, we use ROC-AUC values as a measure of performance. Also in these experiments we adopt the scaffold splitting.

#### 4.1.2 Choices of the Main Models

We test GWMs on various GNN models. Neural Fingerprint (NFP) [5] and Weavenet [10] are relatively classical architectures. A Gated Graph Neural Network (GGNN) [15] is a strong GRU-based GNN. Renormalized Spectral Graph Convolutional Network (RSGCN<sup>1</sup>) [12] is a representative model of the Graph convolutional networks (GCNs). RGAT [2] uses multiple attention mechanisms for a set of edge types. Our implementation of RGAT is slightly different from [2] in the edge-type parameterization and handling of self-links. For further details, please see the appendix. Graph Isomorphism Network (GIN) [30] is one of the newest GNN models. We implement the most simple GIN: 2-layer MLP with ReLU activation for each layer and a bias parameter  $\epsilon$  fixed at 0. We implement GIN with dropout [22], instead of batch-normalization [9].

#### 4.1.3 Implementations and Hyperparameters

We implement all models in Chainer [24] and Chainer-Chemistry<sup>2</sup>, an extension library of the Chainer for chemical data analysis. We conducted a total of three sets of experiments. In the first set of the experiments, we observed the effect of the GWM on the training loss reduction and the test loss reduction for all combinations of four datasets with the four GNN models used in Fig. 1. Also, we conducted an ablation study to test the effect of each component of the GWM. Finally, we made assessment for the effect of the addition of a GWM on the sheer representation power of the model family. In order to compare the GWM-augmented GNNs against their vanilla GNN counterparts on fair grounds, we allowed each model to use the optimal set of hyperparameters, including the number of layers and the dimension of node feature vectors. However, we set the number of heads in all multi-head attention mechanisms to  $K = 8$ , and used  $R = 4$  edge types for the multi-relational mechanism in all models. Also, at every layer, we set the dimension of the supernode feature to be the same as that of the features of the nodes in the main GNN.

Throughout, all models were trained with Adam [11] with  $\alpha = 0.001$ ,  $\beta_1 = 0.9$ , and  $\beta_2 = 0.999$ . At all times, we reported the results of the model snapshots of the epoch at which the best validation score was achieved.

#### 4.2 Training and Test Loss Reduction

A brief peek of the results in the introduction shows that the installment of GWM can improve the representation power of the GNN for the classification task on the Tox21 dataset. We repeat similar experiments for 16 combinations of models and tasks<sup>3</sup>, and report the average  $\bar{r}$  of the loss reduction

<sup>1</sup>The authors do not specify the name of the architecture. Referred as RSGCN in Chainer-Chemistry package.

<sup>2</sup><https://github.com/pfnet-research/chainer-chemistry>

<sup>3</sup>The number of layers and the vector dimensions are fixed for each dataset. For each combination we conduct 10 random runs.

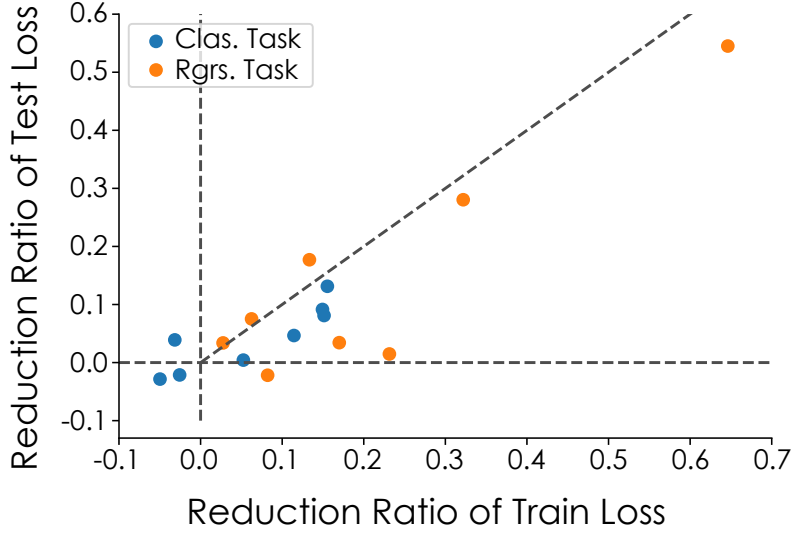


Figure 4: Train and test loss reduction ratios on various pairs of vanilla GNN models and graph datasets. Each plot presents the rational train/test loss reductions induced by the GWM attachment for a specific pair of (dataset, GNN). Averaged over 10 random runs. The horizontal axis denotes the ratio of reduced training loss, and the vertical axis denotes that of the test loss.

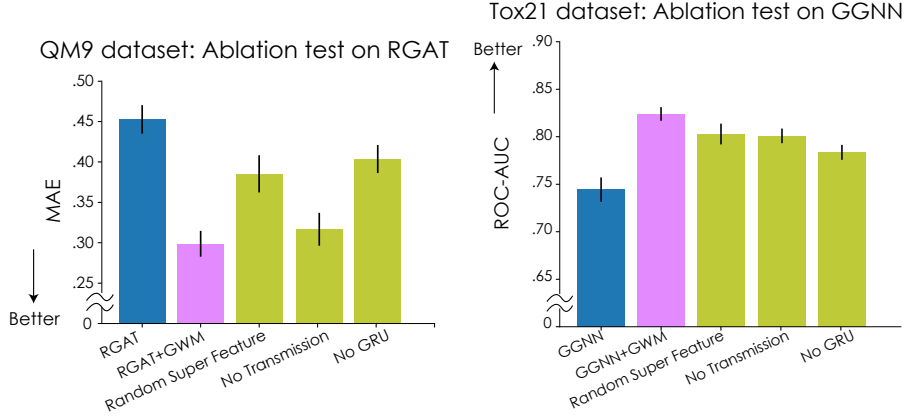


Figure 5: Left: Mean MAEs and the standard deviations for the ablation test on the QM9 dataset with the RGAT model. Right: Mean ROC-AUCs and the standard deviations of the ablation test on the Tox21 dataset with the GGNN model.

ratio  $r = \frac{\mathcal{L} - \mathcal{L}^{(+)}}{\|\mathcal{L}\|}$  for both training loss and test loss.  $\mathcal{L}$  denotes the loss of the vanilla model, and  $\mathcal{L}^{(+)}$  denote the loss of the GWM-installed model. Fig. 4 is the scatter plot of the  $(\bar{r}_{train}, \bar{r}_{loss})$ , with the dotted slope representing  $\bar{r}_{train} = \bar{r}_{loss}$ . As we can see in the plot,  $\bar{r}_{train}$ s are positive for all experiments except for the three (HIV for GGNN, NFP, and RSGCN), which report negative values of minuscule scale ( $\sim 1e-2$ ). This suggests that the representation power improves for almost all pairs of tasks and models. For 12/13 combinations, the generalization performances (test loss) improve as well. The point in the fourth quadrant can be considered as an case of overfitting, in which the reduction of the training loss lead to the increase of the test loss. It is worthy to note that  $\bar{r}_{train}$  and  $\bar{r}_{test}$  are positively correlated in this scatter plot. The result of this experiment thus suggests that our GWM has a general effect of improving the generalization performance through the promotion of the representation power of the original model.



Dataset	GNN model	NFP	WeaveNet	RGAT	GGNN	RSGCN	GIN
LIPO	vanilla GNN	.572 (.030)	1.247 (.445)	.656 (.065)	.517 (.031)	.648 (.027)	.710 (.040)
	+GWM	<b>.554</b> (.031)	<b>.659</b> (.166)	<b>.522</b> (.034)	<b>.455</b> (.021)	<b>.594</b> (.057)	<b>.557</b> (.029)
QM9	vanilla GNN	<b>.371</b> (.012)	.221 (.015)	.439 (.026)	.237 (.022)	.562 (.022)	.380 (.022)
	+GWM	.376 (.022)	<b>.219</b> (.025)	<b>.312</b> (.039)	<b>.232</b> (.017)	<b>.375</b> (.019)	<b>.365</b> (.023)

Table 1: MAEs on the LIPO dataset and QM9 dataset. The number of layers and the dimension of the feature vectors are defined via Bayesian Optimization for each method and each dataset. Averages (standard deviations) over 10 random runs. Smaller values are better.

### 4.3 Ablation test

We test the individual effect of three constituents of GWMs. Firstly, we conduct an ablation test for the effect of the initialization of the supernode by replacing the informative  $g_0$  with uninformative  $g_0$  drawn from uniform distribution. Secondly, we assess the effect of replacing the warp gate coefficients  $z$  with fixed values,  $z = 0.0$  ("No Transmission"). The choice of  $z = 0.0$  amounts to allowing the main GNN and the GWM to communicate in the readout layer only. Finally, we assess the effect of the presence of self recurrent units ("No GRU").

The left panel and the right panel of Fig. 5 show the results of the ablation tests with the RGAT and GGNN models, respectively. Overall, we confirm that every component is necessary for the full performance of GWM. Self recurrent unit in particular seem to play an important role in boosting the efficacy of the GWM.

### 4.4 Effect of the GWM on the representation power of model space

In the final set of the experiments, we compare GWM-augmented GNNs against the vanilla GNN counterparts, with the optimized set of hyperparameters. The hyperparameters we speak hereof includes not only the training parameters, but also the number of layers and the dimension of feature vectors. Bayesian optimization is employed to select the best set of hyperparameters for each experiment using a package in Optuna<sup>4</sup>.

Table 1 and Table 2 respectively present the MAEs on the regression task datasets and the ROC-AUCs for the classification task datasets. As we can see in the tables, the generalization performance with the optimal hyperparameters improves for almost all combinations of tasks and models. The result suggests that the representation power of the model space itself improves significantly with the installment of the GWM.

A few words of cautions is in order here. Despite its biochemical significance, not many studies to date evaluate their models on the MoleculeNet, and most of the rare published studies on this dataset present the performance of their models on the random train/validation/test data split, which is significantly easier than the scaffold train/validation/test data split. As one exception, Li et al. [14] report the best test AUC scores on the HIV and the Tox21 dataset for both the scaffold split and the random split. In their report, the AUC scores are better for the random split than for the scaffold split by  $0.07 \sim 0.1$  point. Their scaffold test scores on the HIV and the Tox21 datasets are respectively 0.776 and 0.759. Also, a more recent paper [32] proposes an ensemble method of GNNs and gradient boosts, and records the scaffold AUC score of 0.807 on Tox21 dataset. These scores are still significantly worse than our best scores (0.833 on Tox21 and 0.832 on HIV), which are both the state-of-the-art in the literature to date.

In general, GGNN [15] based models perform better than other models in our experiments. At the same time the classical baselines, NFP and Weavenet, work greatly in comparison to other networks when the installment of GWM is assumed for all models. This suggests that there is no golden standard GNN in the current GNN literature in terms of the representation power.

## 5 Conclusion

For a generic DNN, numerous effective *installable modules* have been proposed for the improvement of the model, either in predictive ability, representation power, or training stability(e.g. [22, 9, 17, 8]).

<sup>4</sup><https://optuna.org/>

Dataset	GNN model	NFP	WeaveNet	RGAT	GGNN	RSGCN	GIN
HIV	vanilla GNN	<b>.790</b> (.039)	.682 (.172)	.750 (.055)	.787 (.045)	.730 (.038)	.759 (.042)
	+GWM	.761 (.061)	<b>.704</b> (.089)	<b>.791</b> (.044)	<b>.832</b> (.015)	<b>.744</b> (.020)	<b>.765</b> (.038)
Tox21	vanilla GNN	.808 (.017)	.793 (.040)	.752 (.023)	.824 (.011)	.793 (.010)	.797 (.013)
	+GWM	<b>.821</b> (.018)	<b>.812</b> (.025)	<b>.828</b> (.018)	<b>.833</b> (.013)	<b>.805</b> (.011)	<b>.808</b> (.016)

Table 2: ROC-AUCs on the HIV dataset and Tox21 dataset. The number of layers and the dimension of feature vectors are defined via Bayesian Optimization for each method and each dataset. Averages (standard deviations) over 10 random runs. Larger values are better.

As an auxiliary module to be installed to a generic GNN, the proposed GWM is a first of its kind. Also, our experimental results show that the GWM can generally improve the representation power of a GNN as well as the generalization performance, agnostic to the network architecture. We would like to emphasize that the choice of the internal structure of GWM is not limited to the ones we described in this study, and that there are possibly numerous ways to construct the GWM or GWM-like module that can be added to GNNs. For example, there is no provable justification for the use of a linear transformation in the transmissions or a bilinear form in the attention coefficients  $\alpha$ . Effective choices and constructions of supernode features are also open to further research. Moreover, we have observed in the experimental results, the effect of the GWM varied across the datasets and GNNs, suggesting that a specific variant of GWMs suits better for a specific tasks. Also, modules that scale up to very large networks may be of interest for many applications. Our study can possibly open an entirely new avenue for the architectural study of GNNs.

## References

- [1] Joan Bruna and Arthur Szlam. Spectral Networks and Deep Locally Connected Networks on Graphs. In *Proc. ICLR*, 2014.
- [2] Dan Busbridge, Dane Sherburn, Pietro Cavallo, and Nils Y. Hammerla. Relational Graph Attention Networks. *OpenReview*, 2018.
- [3] Kyunghyun Cho, Bart Van Merriënboer, Caglar Gulcehre, Dzmitry Bahdanau, Fethi Bougares, Holger Schwenk, and Yoshua Bengio. Learning phrase representations using rnn encoder-decoder for statistical machine translation. In *Proc. EMNLP*, 2014.
- [4] Jacob Devlin, Ming-wei Chang, Kenton Lee, and Kristina Toutanova. BERT: Pre-training of Deep Bidirectional Transformers for Language Understanding. *arXiv*, page 1810.04805v1 [cs.CL], 2018.
- [5] David Duvenaud, Dougal Maclaurin, Jorge Aguilera-Iparraguirre, Rafael Gómez-Bombarelli, Timothy Hirzel, Alán Aspuru-Guzik, and Ryan P. Adams. Convolutional Networks on Graphs for Learning Molecular Fingerprints. In *Proc. NeurIPS*, 2015.
- [6] Justin Gilmer, Samuel S. Schoenholz, Patrick F. Riley, Oriol Vinyals, and George E. Dahl. Neural Message Passing for Quantum Chemistry. In *Proc. ICML*, 2017.
- [7] Will Hamilton, Zhitao Ying, and Jure Leskovec. Inductive representation learning on large graphs. In *Proc. NeurIPS*, 2017.
- [8] Kaiming He, Xiangyu Zhang, Shaoqing Ren, and Jian Sun. Deep Residual Learning for Image Recognition. In *Proc. CVPR*, 2016.
- [9] Sergey Ioffe and Christian Szegedy. Batch Normalization: Accelerating Deep Network Training by Reducing Internal Covariate Shift. In *Proc. ICML*, 2015.
- [10] Steven Kearnes, Kevin McCloskey, Marc Berndl, Vijay Pande, and Patrick Riley. Molecular graph convolutions: moving beyond fingerprints. *Journal of Computer-Aided Molecular Design*, 30(8):595–608, 2016.
- [11] Diederik P. Kingma and Jimmy Lei Ba. Adam: a Method for Stochastic Optimization. In *Proc. ICLR*, 2015.

- [12] Thomas N. Kipf and Max Welling. Semi-supervised Classification with Graph Convolutional Networks. In *Proc. ICLR*, 2017.
- [13] Alex Krizhevsky, Ilya Sutskever, and Geoffrey E Hinton. ImageNet Classification with Deep Convolutional Neural Networks. In *Proc. NeurIPS*, 2012.
- [14] Junying Li, Deng Cai, and Xiaofei He. Learning Graph-Level Representation for Drug Discovery. *arXiv*, pages 1709.03741v2 [cs, LG], 2017.
- [15] Yujia Li, Daniel Tarlow, Marc Brockschmidt, and Richard Zemel. Gated Graph Sequence Neural Networks. In *Proc. ICLR*, 2016.
- [16] Minh-Thang Luong, Hieu Pham, and Christopher D. Manning. Effective Approaches to Attention-based Neural Machine Translation. In *Proceedings of the 2015 Conference on Empirical Methods in Natural Language Processing (EMNLP)*, pages 1412–1421, 2015.
- [17] Takeru Miyato, Toshiki Kataoka, Masanori Koyama, and Yuichi Yoshida. Spectral Normalization for Generative Adversarial Networks. In *Proc. ICLR*, 2018.
- [18] Raghunathan Ramakrishnan, Pavlo O. Dral, Matthias Rupp, and O. Anatole von Lilienfeld. Quantum chemistry structures and properties of 134 kilo molecules. *Scientific Data*, 1:140022, 2014.
- [19] Lars Ruddigkeit, Ruud van Deursen, Lorenz C. Blum, and Reymond Jean-Louis. Enumeration of 166 billion organic small molecules in the chemical universe database gdb-17. *Journal of chemical information and modeling*, 52(11):2864–2875, 2012.
- [20] Michael Schlichtkrull, Thomas N. Kipf, Peter Bloem, Rianne van den Berg, Ivan Titov, and Max Welling. Modeling Relational Data with Graph Convolutional Networks. *arXiv*, page 1703.06103v4 [stat.ML], 2017.
- [21] Chao Shang, Qinqing Liu, Ko-shin Chen, Jiangwen Sun, Jin Lu, Jinfeng Yi, and Jinbo Bi. Edge Attention-based Multi-Relational Graph Convolutional Networks. *arXiv*, page 1802.04944v1 [stat.ML], 2018.
- [22] Nitish Srivastava, Geoffrey Hinton, Alex Krizhevsky, Ilya Sutskever, and Ruslan Salakhutdinov. Dropout: A Simple Way of Prevent Neural Networks from Overfitting. *Journal of Machine Learning Research*, 15:1929–1958, 2014.
- [23] Christian Szegedy, Wei Liu, Yangqing Jia, Pierre Sermanet, Scott Reed, Dragomir Anguelov, Dumitru Erhan, Vincent Vanhoucke, and Andrew Rabinovich. Going Deeper with Convolutions. In *Proc. CVPR*, 2015.
- [24] Seiya Tokui, Kenta Oono, Shohei Hido, and Justin Clayton. Chainer: a Next-Generation Open Source Framework for Deep Learning. In *Proc. W. Machine Learning Systems (LearningSys) in NeurIPS*, 2015.
- [25] Aaron van den Oord, Sander Dieleman, Heiga Zen, Karen Simonyan, Oriol Vinyals, Alex Graves, Nal Kalchbrenner, Andrew Senior, and Koray Kavukcuoglu. WaveNet: A Generative Model for Raw Audio. *arXiv*, page 1609.03499v2 [cs.SD], 2016.
- [26] Ashish Vaswani, Noam Shazeer, Niki Parmar, Jakob Uszkoreit, Llion Jones, Aidan N. Gomez, Lukasz Kaiser, and Illia Polosukhin. Attention Is All You Need. In *Proc. NeurIPS*, 2017.
- [27] Petar Veličković, Guillem Cucurull, Arantxa Casanova, Adriana Romero, Pietro Liò, and Yoshua Bengio. Graph Attention Networks. In *Proce. ICLR*, 2018.
- [28] Zhenqin Wu, Bharath Ramsundar, Evan N Feinberg, Joseph Gomes, Caleb Geniesse, Aneesh S Pappu, Karl Leswing, and Vijay Pande. MoleculeNet : A Benchmark for Molecular Machine Learning. *Chemical Science*, 9(2):513–530, 2018.
- [29] Zonghan Wu, Shirui Pan, Fengwen Chen, Guodong Long, Chengqi Zhang, Senior Member, and Philip S Yu. A Comprehensive Survey on Graph Neural Networks. *arXiv*, page 1901.00596v1 [cs.LG], 2019.

- [30] Keyulu Xu, Weihua Hu, Jure Leskovec, and Stefanie Jegelka. How Powerful are Graph Neural Networks? *arXiv*, page 1810.00826v2 [cs.LG], 2018.
- [31] Rex Ying, Jiaxuan You, Christopher Morris, Xiang Ren, William L. Hamilton, and Jure Leskovec. Hierarchical Graph Representation Learning with Differentiable Pooling. In *Proc. NeurIPS*, 2018.
- [32] Mikhail Zaslavskiy, J Simon, Eric W Tramel, and Gilles Wainrib. ToxicBlend : Virtual Screening of Toxic Compounds with Ensemble Predictors. *arXiv*, page 1806.04449 [stat.ML], 2018.
- [33] Jie Zhou, Ganqu Cui, Zhengyan Zhang, Cheng Yang, Zhiyuan Liu, and Maosong Sun. Graph Neural Networks : A Review of Methods and Applications. *arXiv*, page 1812.08434v2 [cs.LG], 2018.

## A Our formulation of RGAT

Apart from the original RGAT [2], we have developed a similar GNN in a slightly different formulation. Followings are our RGAT formulation:

$$h_{\ell+1,i} = \tanh \left( W_i \text{concat}_{k=1}^K \tilde{h}_{\ell,i,k} \right), \quad (13)$$

$$\tilde{h}_{\ell,i,k} = F_{\ell,k} h_{\ell,i} + \sum_{j \in N_i} \alpha_{i,j,k} G_{\ell,k} h_{\ell,j}, \quad (14)$$

$$\alpha_{i,j,k} = \text{softmax} \left( a \left( h_{\ell,i}, h_{\ell,j}; A_{\ell,k,e_{i,j}} \right) \right). \quad (15)$$

$W, F, G, A$  are the coefficient matrix to be tuned.  $\ell$  is the index of the layer up to  $L$ ,  $k$  is the index of the attention head up to  $K$ ,  $i, j$  are the index of the nodes up to  $N$ ,  $e_{i,j} = r$  is the index of the edge type up to  $R$ .

The main point is the edge type information in Eq.16. The edge type  $e_{i,j} = r$  switches the weight matrix of the attention similarity function,  $a$ . This means that the associations between nodes should be computed dependent on the edge type. This is a natural assumption for chemical molecular graphs. Typically we have multiple bond types between nodes = atoms: single-bond, double-bound, triple-bond, and the aromatic ring. It is natural to assume that interactions between atoms are affected by the bond types among the atoms.

The main differences from the original RGAT lie in the Eq.14. The original RGAT assumes that the weight matrix  $G$  is also dependent on the edge type ( $G_{\ell,k,e_{i,j}}$ ) while we omit this dependency. Also, the original RGAT does not provide a self-link weight matrix  $F$  while we do. We made these changes based on our preliminary experiments. We found our formulation is better than the original RGAT formulation in the MoleculeNet dataset, in terms of the training stabilities and the generalization performances.

Another difference is the choice of the attention function. In our formulation, the attention similarity measure  $a(\cdot)$  is defined by the *general* attention in [16] while the original GAT [27] and the RGAT [2] employed a simpler *concat* attention:

$$a \left( h_{\ell,i}, h_{\ell,j}; A_{\ell,k,e_{i,j}} \right) = h_{\ell,i}^T A_{\ell,k,e_{i,j}} h_{\ell,j}. \quad (16)$$

## B Experiments Details

### B.1 Graph Data Representation

All datasets used in our experiments are taken from the MoleculeNet[28]. Four used datasets are provided in the SMILES format. A SMILES format is a line notation for describing the structure of chemical compounds. We decode a SMILES molecular data into a graph representation of the molecule. A node in the graph corresponds to an atom. Each atom node is associated with the symbolic label of the atom name ("H", "C", ...). An edge in the graph corresponds to a bond between atoms. Each bond edge is associated with the bond type information (single-, double-, ....).

Given the graph, we extract input feature vectors for node  $x_i$  and that of supernode  $x'$ .  $x_i$ , the input feature vector for the node  $i$  is a  $D$ -dimensional continuous vector, which is an embedded vector of the one-hot atom label vector with a trainable linear transformation.  $X'$ , The input feature vector for the supernode is a  $D'$ -dimensional continuous vector, which again is an embedded vector of some graph-global features with a trainable linear transformation. Choices for the graph-global features are detailed in the following section.

The edge information is converted in an adjacency matrix,  $\mathcal{A}$ .

## B.2 Explicit Features for Supernode

Since the supernode does not exist in the original graph  $G$ , we have no observable cues for the supernode. For simplicity, we propose to use an aggregation of node features, such as:

- Histograms of discrete labels attached to original nodes
- Averages, maximums, minimums, or medians of numerical attributes attached to original nodes
- Histograms of edge types if the graph is multiple relational graph.
- Number of nodes, graph diameters, modularity, and other simple statistics for graph structure.

We can augment the super feature vector  $x'$  if some additional information about the graph is provided. Essentially, these simple aggregations of the feature vectors do not bring new information into the network. However we found that the graph-wise super feature input boosts the performance of the learned network model.

## B.3 Data splits

In chemical datasets, a totally random shuffling of samples into train/val/test subsets is not always a valid way of data splitting. Therefore MoleculeNet provides several ways of data splitting. The "random" split is the random sample shuffling that are most familiar to the machine learning community. The "scaffold" split separate samples based on the molecular two-dimensional structure. Since the scaffold split separates structurally different molecules into different subsets, "it offers a greater challenge for learning algorithms than the random split" [28].

Throughout the paper, we adopt the scaffold split to assess the full potential of the GWM-attaching GNNs.

## B.4 Readout Layer

In many applications of GNNs users may expect a single fixed-length vector representing the characteristics of the graph  $G$ . So we add the 'readout' layer to aggregate the local node hidden states  $\{H_\ell\}$  and the global node hidden states  $\{g_\ell\}$ .

A main issue in the readout unit is how to aggregate the local nodes, whose number varies for each graph. A simple way is to take an arithmetic average (sum) of the  $h$ s at the  $L$ -th layer, but we can also use a DNN to compute (non-linear) "average" of  $h$ s [15, 6]. After the aggregation of the local node hidden states, we simply concatenate it with  $g$ s and apply some transformations to achieve the readout vector,  $r$ :

$$r = \text{DNN}_{r1} (\text{concat} [\text{DNN}_{r2} (H_L), g_L]) . \quad (17)$$

## B.5 Hyperparameters and Other Details

We list the hyperparameters (the number of layers  $L$ , the dimension of feature vectors  $D(= D')$ ) used in several experiments/figures, as well other experimental/implementation details.

### B.5.1 Figure 1: Training Loss over $L$ and $D$

For the experiments on Figure 1 in the main manuscript, we used the Tox21 dataset.

Dataset	GNN model	NFP	WeaveNet	RGAT	GGNN	RSGCN	GIN
LIPO	vanilla GNN	(3, 50)	(3, 50)	(3, 50)	(3, 50)	(3, 50)	(3, 190)
	+GWM	(2, 225)	(3, 40)	(3, 31)	(6, 127)	(4, 22)	(4, 257)
QM9	vanilla GNN	(7, 176)	(3, 200)	(5, 14)	(6, 130)	(3, 154)	(3, 199)
	+GWM	(5, 100)	(3, 150)	(2, 71)	(3, 250)	(5, 163)	(5, 163)
HIV	vanilla GNN	(2, 144)	(3, 33)	(2, 12)	(2, 58)	(6, 22)	(2, 66)
	+GWM	(5, 150)	(3, 50)	(2, 15)	(2, 40)	(5, 27)	(2, 80)
Tox21	vanilla GNN	(5, 382)	(7, 485)	(3, 200)	(4, 231)	(2, 160)	(3, 161)
	+GWM	(4, 290)	(4, 58)	(4, 109)	(3, 48)	(5, 40)	(2, 245)

Table 3: Hyperparameters  $L$  and  $D$  for the experiment in Section 4.4. The format of the table cells is:  $(L, D)$ .

To study the effect of the number of layers  $L$  (the left panel), we fixed the dimension  $D = 32$ . To study the effect of the feature vector dimensions  $D$  (the right panel), we fixed the number of layers  $L = 4$ .

All models are trained for 30 epochs.

### B.5.2 Section 4.2: Train/Test Loss Reduction

In the experiment in the Section 4.2 (Figure 4 in the main manuscript), we used four datasets. For each dataset, we fixed  $L$  and  $D$  for all GNN models to compare the loss reduction performances. For the Tox21 dataset, we set:  $L = 4$ ,  $D = 32$ . For the HIV dataset, we set:  $L = 4$ ,  $D = 100$ . For the LIPO dataset, we set:  $L = 3$ ,  $D = 50$ . For the QM9 dataset, we set:  $L = 4$ ,  $D = 100$ .

All models were trained for 30 epochs.

### B.5.3 Section 4.3: Ablation Test

For the ablation test on the Tox21 dataset, we adopted  $L = 4$ ,  $D = 32$ . For the ablation test on the QM9 dataset, we adopted  $L = 3$ ,  $D = 200$ .

All models were trained for 30 epochs.

### B.5.4 Section 4.4: the full comparison

For the experiments in the Section 4.4 (Table 1 and 2 in the main manuscript), we employed the Bayesian optimization to tune  $L$  and  $D$  for each combinations of a dataset and a GNN model. The Bayesian optimization trials were conducted by the Optuna library, with 50 sampling (searches) for each combination. Chosen  $L$ s and  $D$ s are presented in the Table 3.

For the QM9 dataset, we trained the models for 50 epochs. For the HIV and the Tox21 dataset, we trained the models for 100 epochs. For the LIPO dataset, we trained the models for 200 epochs.